Journal of
Marine Science and Engineering

MDPI

Article

The Hydrodynamic Dispersion Characteristics of Coral Sands

Xiang Cui [1,2], Changqi Zhu [1,*], Mingjian Hu [1], Xinzhi Wang [1] and Haifeng Liu [1]

[1] State Key Laboratory of Geomechanics and Geotechnical Engineering, Institute of Rock and Soil Mechanics, Chinese Academy of Sciences, Wuhan 430071, China
[2] University of Chinese Academy of Sciences, Beijing 100049, China
* Correspondence: cqzhu@whrsm.ac.cn

Received: 10 July 2019; Accepted: 24 August 2019; Published: 28 August 2019

Abstract: Dispersion characteristics are important factors affecting groundwater solute transport in porous media. In marine environments, solute dispersion leads to the formation of freshwater aquifers under islands. In this study, a series of model tests were designed to explore the relationship between the dispersion characteristics of solute in calcareous sands and the particle size, degree of compactness, and gradation of porous media, with a discussion of the types of dispersion mechanisms in coral sands. It was found that the particle size of coral sands was an important parameter affecting the dispersion coefficient, with the dispersion coefficient increasing with particle size. Gradation was also an important factor affecting the dispersion coefficient of coral sands, with the dispersion coefficient increasing with increasing d_{10}. The dispersion coefficient of coral sands decreased approximately linearly with increasing compactness. The rate of decrease was −0.7244 for single-grained coral sands of particle size 0.25–0.5 mm. When the solute concentrations and particle sizes increased, the limiting concentration gradients at equilibrium decreased. In this study, based on the relative weights of molecular diffusion versus mechanical dispersion under different flow velocity conditions, the dispersion mechanisms were classified into five types, and for each type, a corresponding flow velocity limit was derived.

Keywords: coral sands; porous media; model test; dispersion; mechanical dispersion; molecular diffusion

1. Introduction

Coral sands are a kind of biogenic soil in marine environments, originating from the fracturing and sedimentation of coral skeletons by wind and waves [1]. The primary features of coral sands include a high content of calcium carbonate—often more than 90%—and a relatively short sediment transport distance, which results in particles frequently retaining the inner pore structure of coral bones, and are characterized by irregular shapes, high angularity, and fragility [2–4]. The sediments formed by coral sands have a high void ratio and display hydrogeological characteristics different from those of terrigenous sediments. Islands in the South China Sea are all composed of coral sediments, with these sediments being the only carriers in the formation of fresh groundwater aquifers in the South China Sea islands and reefs. Given that the dispersion coefficient of coral sands is a key factor affecting the conservation of fresh groundwater, uncovering the dispersion pattern of groundwater solute in coral sands will provide the basic parameters and theoretical basis for the numerical simulation of the formation and evolution of fresh groundwater aquifers in the South China Sea islands and reefs, as well as the conservation and utilization of these aquifers.

Solute dispersion in hydrated porous media has been extensively studied. The earliest work was performed by Taylor, who used a capillary tube model to investigate this topic and proposed a method

for calculating the longitudinal dispersion coefficient of porous media [5]. Taylor considered only convection, and therefore derived the molecular diffusion coefficient by measuring the longitudinal dispersion coefficient [5]. Klotzd et al. explored the relationship between the longitudinal dispersion coefficient and average pore flow velocity, the fluid viscosity coefficient, and the characteristic parameters of soil media by conducting a large number of field and laboratory experiments [6]. Gupta proposed a solute transport mechanism for unsaturated porous media, suggesting that two types of pores exist in unsaturated soils, namely, "backbones" and "dead ends," with solute mainly moving by convection in the former and by diffusion in the latter [7]. De Arcangelis et al. studied dispersion calculation methods for network models of porous media, deduced the precise law of tracer motion under the combined action of molecular diffusion and convection, and introduced an effective probability propagation algorithm, which permitted an exact calculation of the distribution of the first-passage-time of the tracer as it flowed through the medium [8]. Sahimi studied hydrodynamic dispersion in two types of heterogeneous porous media, one in which a fraction of the pores did not allow material transport to take place, and the other in which the permeabilities of various regions of the pore space were fractally distributed [9]. Lowe calculated the dispersion coefficient of tracer particles in the fluid of a porous medium randomly filled with spheres, finding that at high Peclet numbers, the tracer motion was mainly determined by convection, and the dispersion process was abnormal with a divergent dispersion coefficient [10]. Zhang proposed a calculation method for hydrodynamic dispersion parameters of adsorptive solutes, deriving formulas for calculating hydrodynamic dispersion coefficients of saturated and unsaturated soils [11]. LI improved the flexible-wall permeameter to make it suitable for finding the dispersion parameters of low-permeability soils, namely, determining the dispersion coefficients through numerical inversion of the breakthrough curve [12]. Shao conducted a one-dimensional dispersion test with silt loam, calculated the hydrodynamic dispersion coefficient of unsaturated silty loam using the soil water and salt dynamics measured in a vertical soil column solute transport experiment, and established the relationship between hydrodynamic dispersion coefficients and pore flow velocities for this type of soil [13]. Jensen adopted the nonlinear least-squares optimization code CXTFIT developed by Parker and van Genuchten to perform curve fitting, thereby obtaining parameters for different forms of the convection–dispersion equation (CDE) [14].

The underground freshwater of islands are the basis for the normal operation of their ecosystems. The generation of underground fresh water is closely related to island size and stratum characteristics. Restricted by the scale of research objects and experimental conditions, the research in this aspect is mostly conducted by means of numerical simulation. The permeability coefficient, dispersion coefficient, and specific yield are three important parameters that must be assigned to strata in numerical simulations. All three parameters can be obtained using field tests. However, the data obtained represent only the island studied, and are not universally representative. In addition, the artificial islands in the South China Sea are not open to the public, making it difficult to conduct field experiments there. In our study, with coral sands as the research subject, which have different granular morphologies and sediment characteristics than terrigenous sediments, laboratory model tests were employed to uncover the dispersion mechanisms of groundwater solute in coral sands, as well as the main factors influencing these mechanisms. According to the results of our study, the empirical value of dispersion coefficients can be provided for calcareous soils with common gradation and compactness. In this way, a more stratigraphic collocation design can be considered in the numerical simulation, so as to find the optimal stratigraphic design scheme that can promote the formation of underground fresh water.

In addition, the study of hydrodynamic dispersion presented in this paper can also be applied to many other aspects. In the simulation and prediction of groundwater pollution, the dispersion coefficient is an important parameter needed for simulation, which provides a quantitative basis for groundwater resource management and groundwater pollution reconstruction. Regarding the intrusion of seawater into coastal aquifers, the study of hydrodynamic dispersion is helpful in studying the migration of the transition zone of brackish water. In terms of water and salt transport in the

vade-zone, the study of hydrodynamic dispersion is helpful in solving the problem of the effect of fertilizers and pesticides on underground water quality in islands. Finally, in terms of sewage treatment, hydrodynamic dispersion is helpful in solving the problem of the impact of sewage discharge from living and production on the underground freshwater quality in islands.

2. Test Scheme

The coral sands used for testing were taken from a natural reef in the South China Sea, whose gradation characteristics are shown in Figure 1. The coefficient of curvature C_c was 2.12, which is within the range of 1–3. The coefficient of uniformity C_u was 45.45, which is much greater than 5, indicating that the reef consisted of a type of coral sand with good gradation. The coral sand was screened to obtain six kinds of coral sand with a single particle size, as shown in Figure 2. More specifically, the test scheme was composed of three steps: (1) using a self-designed one-dimensional dispersion test device, solute dispersion tests were conducted on a total of 14 groups of coral sands of a single particle size and dry density under various conditions to explore how the dispersion coefficient varies as a function of particle size and dry density; (2) using a custom-designed pore tortuosity test device, where pore tortuosity tests were conducted on a total of five groups of coral sands of a single particle size under various conditions to explore how the pore tortuosity varies as a function of particle size; and (3) using a custom-designed molecular diffusion and mechanical dispersion test device, where for a total of six test groups, molecular diffusion tests were conducted with different concentrations of injected solutions under the condition of the pore fluid having a flow velocity. In addition, molecular diffusion and mechanical dispersion tests were conducted with pore flow velocity increasing in a stepwise manner in order to explore how the weight of molecular diffusion versus mechanical diffusion varies with a stepwise increase in pore flow velocity. The test scheme is shown in Table 1.

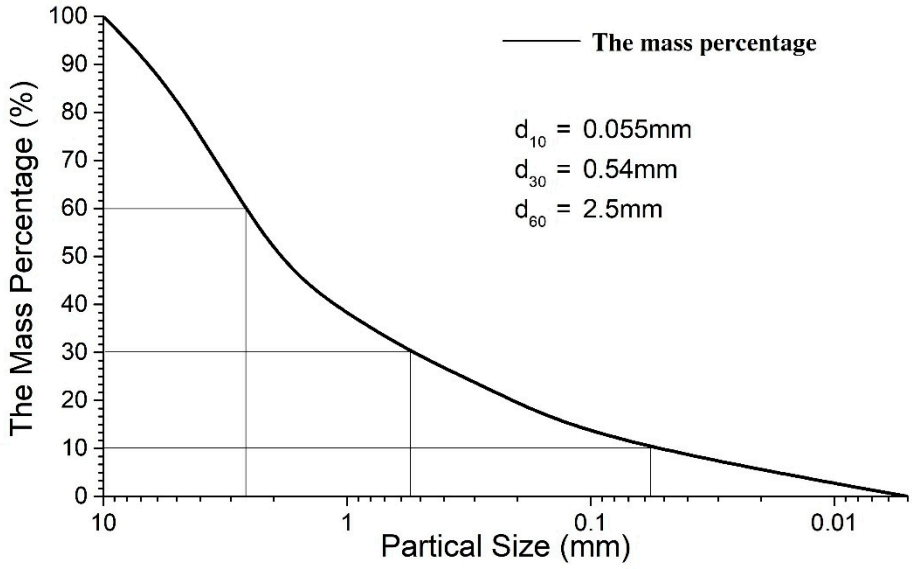

Figure 1. Gradation curve of coral sands used in the tests.

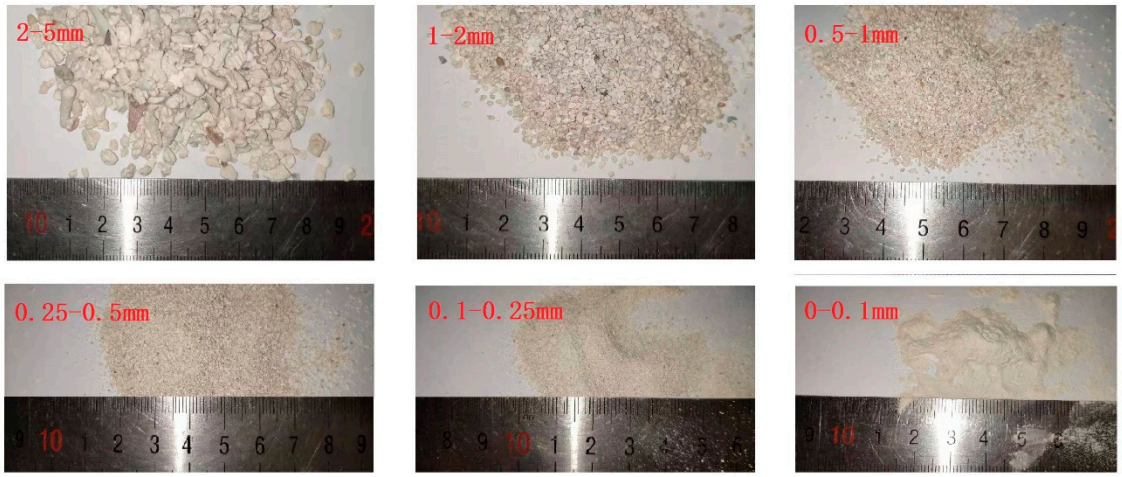

Figure 2. Calcareous sand of various grain sizes.

Table 1. Test scheme.

Test 1: One-Dimensional Dispersion Test			
Group	**Gradation**	**Dry Density (g/cm^3)**	**C (NaCl) (g/L)**
1	0–0.1 mm (100%)	1.3	20
2	0.1–0.25 mm (100%)	1.3	20
3	0.25–0.5 mm (100%)	1.3	20
4	0.5–1 mm (100%)	1.3	20
5	1–2 mm (100%)	1.3	20
6	2–5 mm (100%)	1.3	20
7	0.25–0.5 mm (100%)	1.2	20
8	0.25–0.5 mm (100%)	1.3	20
9	0.25–0.5 mm (100%)	1.4	20
10	No.1 (d_{60} = 2.5, d_{30} = 0.52, d_{10} = 0.05)	1.3	20
11	No.2 (d_{60} = 2.5, d_{30} = 0.52, d_{10} = 0.15)	1.3	20
12	No.3 (d_{60} = 2.5, d_{30} = 0.6, d_{10} = 0.31)	1.3	20
13	No.4 (d_{60} = 2.5, d_{30} = 0.9, d_{10} = 0.6)	1.3	20
14	No.5 (d_{60} = 2.55, d_{30} = 1.5, d_{10} = 1.2)	1.3	20
Test 2: Pore Tortuosity Test			
Group	**Gradation**	**Dry Density (g/cm^3)**	**C (NaCl) (g/L)**
1	0–0.1 mm (100%)	1.3	20
2	0.1–0.25 mm (100)	1.3	20
3	0.25–0.5 mm (100%)	1.3	20
4	0.5–1 mm (100%)	1.3	20
5	1–2 mm (100%)	1.3	20
Test 3: Molecular Diffusion and Mechanical Dispersion Tests			
Group	**Gradation**	**Flow Velocity (cm/s)**	**Dry Density (g/cm^3)**	**C (NaCl) (g/L)**
1	0.25–0.5 mm (100%)	0	1.3	20
2	0.25–0.5 mm (100%)	0	1.3	60
3	0.25–0.5 mm (100%)	1.36×10^{-4}	1.3	60
4	0.25–0.5 mm (100%)	6.61×10^{-4}	1.3	60
5	0.25–0.5 mm (100%)	1.60×10^{-3}	1.3	60
6	0.25–0.5 mm (100%)	6.16×10^{-3}	1.3	60

3. Test Method

3.1. One-Dimensional Dispersion Test

The hydrodynamic dispersion coefficient is a tensor related to the average pore velocity and the characteristics of the porous medium. Studies show that the dispersion is directional even in an isotropic medium and is more complex when the medium is anisotropic [15]. Given this information, only the one-dimensional dispersion characteristics of a solute in coral sands were explored in this study. The test was conducted with a custom-designed one-dimensional dispersion test device, as shown in Figure 3. The complete test device consisted of four parts (denoted by numbers in the figure): dispersion columns (01), a freshwater supply tank (02), a tracer supply tank (03), and a data acquisition system (04). The dispersion columns were composed of several organic glass columns; each column was 8 cm in inner diameter and 50 cm in height. The preparation and tests of the porous medium samples were performed in the dispersion columns, with a 5-cm-thick buffer layer of glass beads placed separately at the top and bottom of the samples. The sensors used in the data acquisition system were CS655 multi-parameter sensors (Campbell Scientific, State of California, America), which can simultaneously measure volumetric moisture content, temperature, conductivity, dielectric constant, signal propagation time, and signal attenuation. The tracer was a 20 g/L NaCl solution and the samples were single-grained coral sands. The test was conducted by continuously injecting the tracer and collecting the data at a fixed location. The samples in the dispersion columns were first saturated with fresh water, then the valve of the freshwater supply tank was shut, followed by opening the valve of the tracer supply tank and starting data acquisition in a synchronous manner. The relative concentration of NaCl was calculated according to $C = (C_{cj} - C_0)/(C_{max} - C_0)$, with C_{cj} denoting the NaCl concentration at time j. C_0 was the NaCl concentration at the initial time, and C_{max} was the maximum concentration (final steady concentration) in the test.

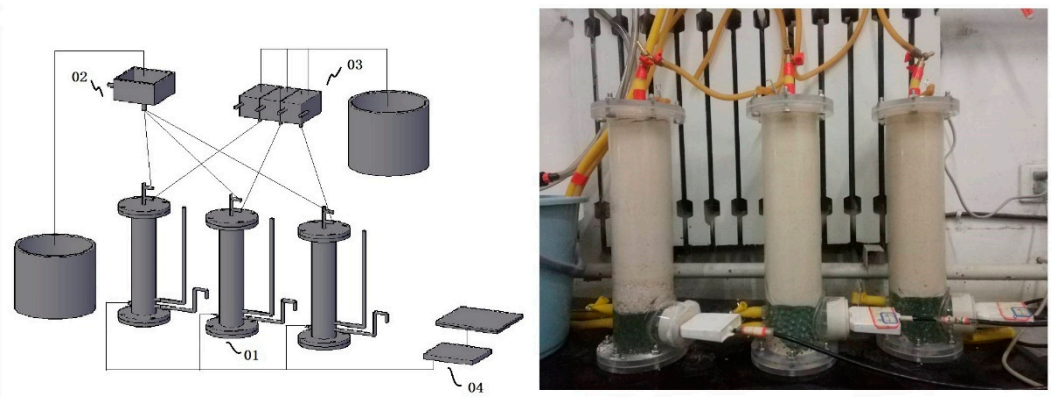

(a) Schematic Diagram (b) Real Product

Figure 3. One-dimensional dispersion device (01: one-dimensional soil column, 02: freshwater supply tank, 03: tracer supply tank, 04: data acquisition system).

The concentration distribution was derived by solving the one-dimensional steady flow problem in a semi-infinite soil column with a constant concentration at one end. With t (s) as the time since the tracer has been turned on, x (cm) as the distance of the multi-parameter sensor from the tracer injection port, $E(x, t)$ (dS/m) as the conductivity measured at time t, E_0 (dS/m) as the conductivity of the tracer, and u (cm/s) as the average flow velocity of the pore fluid in the soil column, the longitudinal dispersion coefficient D_L (cm^2/s) is calculated as given below, and the coordinate system is shown in Figure 4.

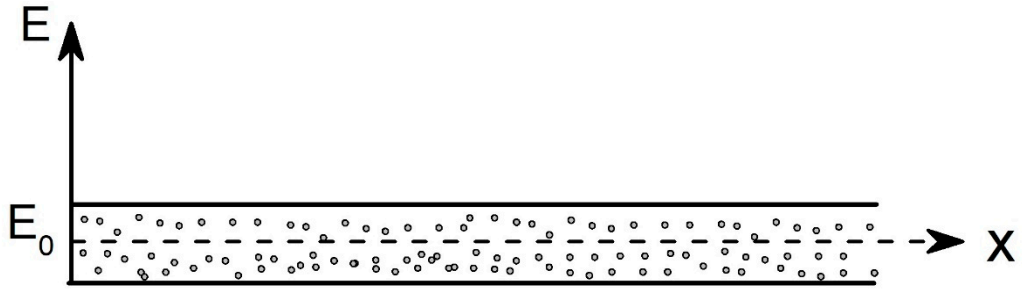

Figure 4. Boundary problem with a constant concentration at one end of the one-dimensional soil column.

The above problem is converted into a mathematical equation as follows:

$$\begin{cases} \frac{\partial E}{\partial t} = D_L \frac{\partial^2 E}{\partial x^2} - u \frac{\partial E}{\partial x} \\ E(x,0) = 0, x \geq 0 \\ E(0,t) = E_0, t > 0 \\ E(\infty,t) = 0, t > 0 \end{cases} \tag{1}$$

The Laplace transform of Equation (1) with respect to t gives

$$\begin{cases} D_L \frac{d^2 \overline{E}}{dx^2} - u \frac{dp\overline{E}}{dx} = p\overline{E} \\ \overline{E}(0,p) = \frac{E_0}{p}, \mathrm{t} > 0 \\ \overline{E}(\infty,p) = 0, \mathrm{t} > 0 \end{cases} \tag{2}$$

where $\overline{E}(x,p)$ is a function of x, and p is a parameter. The original problem is converted into the following definite solution problem as an ordinary differential equation:

$$D_L \frac{d^2 \overline{E}}{dx^2} - u \frac{dp\overline{E}}{dx} - p\overline{E} = 0 \tag{3}$$

The solution of the second-order homogeneous linear ordinary differential equation is:

$$\frac{E(\mathrm{x},\mathrm{t})}{E_0} = \frac{1}{2} erfc\left[\frac{x-ut}{2\sqrt{D_L t}}\right] + \frac{1}{2} e^{\frac{ux}{D_L}} erfc\left[\frac{x+ut}{2\sqrt{D_L t}}\right] \tag{4}$$

where *erfc* is the complementary error function, and ξ in $erfc(u) = 1 - \frac{2}{\sqrt{\pi}} \int_0^{\mathrm{u}} \mathrm{e}^{-\xi^2 d\xi}$ is the mathematical expectation value.

When x or t is large:

$$\frac{E(\mathrm{x},\mathrm{t})}{E_0} = \frac{1}{2} erfc\left[\frac{x-ut}{2\sqrt{D_L t}}\right] = \frac{1}{\sqrt{\pi}} \int_{\frac{\mathrm{x-ut}}{2\sqrt{\mathrm{D_L t}}}}^{\infty} e^{-\varepsilon 2} d\xi \tag{5}$$

Let $\xi^2 = \eta^2/2$ and $\mathrm{d}\xi = 1/\sqrt{2} d\eta$ (where η is the substitute for the mathematical expectation value ξ and does not have practical meaning), then we have:

$$\frac{E(\mathrm{x},\mathrm{t})}{E_0} = 1 - \frac{1}{\sqrt{2\pi}} \int_{-\infty}^{\frac{\mathrm{x-ut}}{\sqrt{2D_L}}} e^{-\frac{\eta^2}{2}} d\eta = 1 - N\left[\frac{x-ut}{\sqrt{2D_L t}}\right] \tag{6}$$

Then, according to Equation (6):

$$0.1587 = 1 - N\left[\frac{x-ut_{0.1587}}{\sqrt{2D_L t_{0.1587}}}\right] 0.8413 = N\left[\frac{x-ut_{0.1587}}{\sqrt{2D_L t_{0.1587}}}\right]$$

According to the normal distribution table, $N(-1) = 0.1587, N(1) = 0.8413$, thereby leading to:

$$\frac{x - ut_{0.1587}}{\sqrt{2D_L t_{0.1587}}} = 1$$

$$\frac{x - ut_{0.8413}}{\sqrt{2D_L t_{0.8413}}} = -1 \quad (7)$$

Solving this equation leads to the dispersion coefficient as follows:

$$\left[\frac{x - ut_{0.1587}}{\sqrt{2D_L t_{0.1587}}} - \frac{x - ut_{0.8413}}{\sqrt{2D_L t_{0.8413}}}\right]^2 = 4 \quad (8)$$

Here, $t_{0.1587}$ is the time when $(C_{cj} - C_0)/(C_{max} - C_0) = 0.1587$ s and $t_{0.8413}$ is the time when $(C_{cj} - C_0)/(C_{max} - C_0) = 0.8413$ s.

3.2. Molecular Diffusion and Pore Tortuosity Tests

Hydrodynamic dispersion is a process that includes molecular diffusion and mechanical dispersion. Molecular diffusion is the process of molecular transport associated with the stochastic movement of molecules due to a concentration gradient. Mechanical dispersion is the process of mechanical mixing that takes place in porous media as a result of the movement of fluid through the pore space. When the average pore flow velocity is 0, dispersion takes the form of molecular diffusion. In this study, each sample consisted of single-grained coral sands, and there was a total of six test groups, with particle sizes ranging from 0–0.1 mm, 0.1–0.25 mm, 0.25–0.5 mm, 0.5–1 mm, and 1–2 mm, while the dry density of each sample was a fixed value: $\rho_d = 1.3$ g/cm^3. The tracer and sensor types were the same as those in the one-dimensional dispersion test. The test instrument was a custom-designed and built molecular diffusion device, as shown in Figure 5. There was a control partition in the middle of the device, and after the partition was lifted, the fluids in the left and right sample box compartments could flow back and forth between the compartments. The sizes of the left and right sample boxes were both 10 cm × 10 cm × 10 cm, and the left sample was saturated with NaCl solution while the right sample was saturated with fresh water. Timing and data reading were started simultaneously with the lifting of the partition.

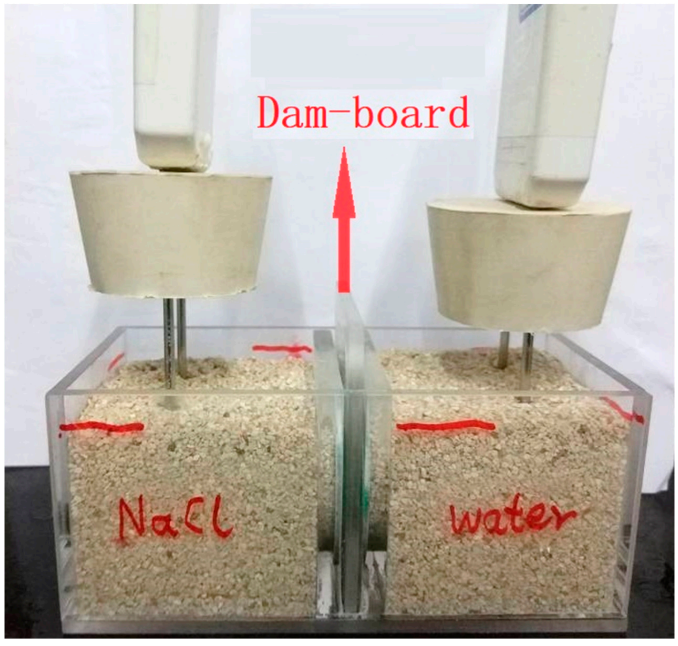

Figure 5. Molecular diffusion and pore tortuosity test device.

Let *EN-t* and *EW-t* be the measured conductivity at time *t* on the left and right sides, respectively, and *EM-t* = (*EN-t* + *EW-t*)/2 be the mean value of the two measured conductivities at time *t*.

3.3. Molecular Diffusion and Mechanical Dispersion Tests

When the pore flow velocity is greater than 0, molecular diffusion and mechanical dispersion processes coexist. With an increase in average pore flow velocity, the weight of molecular diffusion versus mechanical dispersion changes. In order to further study the relationship between the weight and the flow velocity, a custom-designed molecular diffusion and mechanical dispersion test device was employed in this study, as shown in Figure 6. The device consisted of three components, namely, a dispersion body, a water supply part, and a data acquisition system. The dispersion body was made up of organic glass tubes and samples, with each tube being 8 cm in inner diameter and 80 cm in length. The samples were coral sands with particle sizes of 0.25–0.5 mm and a dry density of 1.3 g/cm^3. The data acquisition system was equipped with CS655 multi-parameter sensors; the tracer was a 20 g/cm^3 NaCl solution.

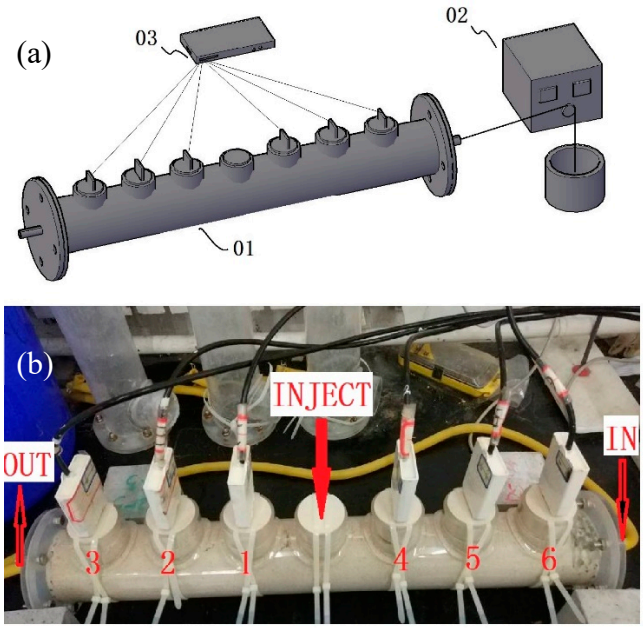

Figure 6. Molecular diffusion and mechanical dispersion test device. (**a**) Schematic Diagram (**b**) Real Product (01: dispersion body, 02: water supply part, 03: data acquisition system).

The required coral sand samples were first prepared in the dispersion tubes. The samples were then saturated with fresh water, after which the inlet and outlet valves of the dispersion tube were shut. The NaCl solution was then injected into the tracer injection port and the injection port was shut. This was completed while simultaneously starting data acquisition, with the pore flow velocity in the device being 0. The above steps were repeated using different concentrations of NaCl solution.

Next, dispersion tests with pore flow velocities greater than 0 were conducted according to the above steps, with the exception that the inlet and outlet valves of the dispersion tube were reopened after the injection of the tracer to allow the pore fluid at a certain flow velocity to pass through the samples. The pore flow velocity was controlled by adjusting the output power of the water pump. By repeating the above test procedure, dispersion tests were performed at several different pore flow velocities.

4. Test Results and Analyses

4.1. Effect of Particle Size on the Dispersion Coefficient

In order to uncover the effect of particle size on the one-dimensional dispersion coefficient, dispersion tests were performed on a total of six groups of single-grained coral sand samples, with the sample groups having a particle sizes of < 0.1 mm, 0.1–0.25 mm, 0.25–0.5 mm, 0.5–1 mm, 1–2 mm, and 2–5 mm; the groups had particle size ranges within the categories of silt, fine sand, medium sand, coarse sand, gravelly sand, and crushed stone (angular gravel), respectively. These groupings were determined according to the soil classification method in the Code for the Investigation of Geotechnical Engineering (GB50021-2001) (Ministry of Construction of the People's Republic of China, 2009) [16]. The dry density of all samples was 1.3 g/cm^3.

Figure 7 presents a one-dimensional dispersion curve for single-grained coral sands, which indicates that when the particle size was 0–0.1 mm, the dispersion process consisted of three stages: a drainage stage, a displacement stage, and a stabilization stage. In the drainage stage, the original saturated fluid in the soil column was discharged outward under the displacement of the tracer, a circumstance in which the discharged fluid had the same concentration as the original saturated fluid, thereby leading to a flat dispersion curve. In the displacement stage, with the continuous injection of the tracer, the tracer underwent diffusion in the original saturated solution, in addition to producing the displacement effect. The diffusion "interface" existed in the form of a concentration transition zone between the original saturated fluid and the tracer. When the edge of the transition zone reached the sensor position, the measured concentration of the discharged fluid began to increase, indicative of the onset of the displacement stage, as manifested by the curve slope starting to increase. In the stabilization stage, when the tracer had completely displaced the original saturated fluid, the discharged fluid had a concentration similar to that of the tracer, with the curve reaching the highest value and tending to flatten.

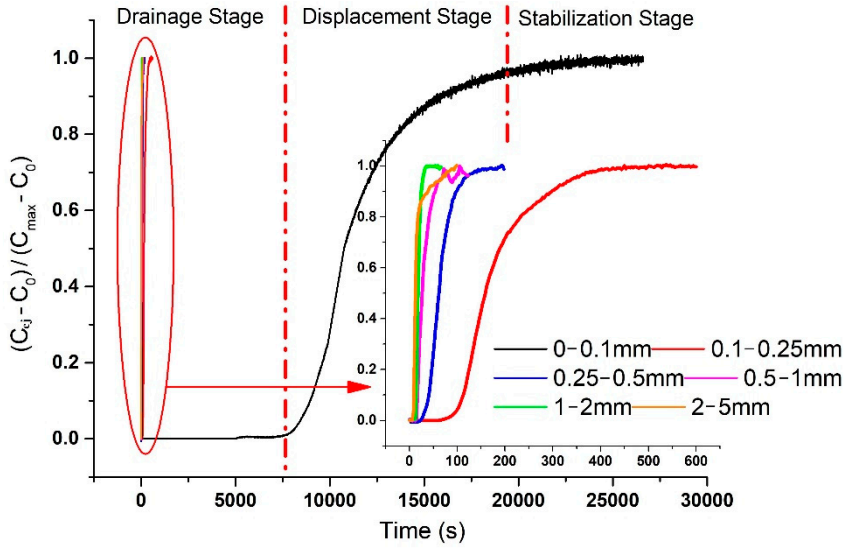

Figure 7. One-dimensional dispersion curves of single-grained coral sands.

As revealed by the above observations, different sample groups of different particle sizes exhibited dispersion pattern similarities, although the drainage stage gradually shortened with increasing particle size. The curve's slope in the displacement stage, i.e., the diffusion rate, increased with increasing particle size, and the time taken for the concentration to reach the stabilization stage gradually shortened with increasing particle size. With the exception of the 0–0.1 mm group, the other three groups were relatively similar to each other in terms of the parameters of the three stages,

indicating a significant difference in dispersion characteristics between the particle size 0–0.1 mm and the other particle sizes.

Figure 8 shows the variation pattern of the one-dimensional dispersion coefficient with respect to particle size. The dispersion coefficient of coral sands increased with increasing particle size. When the particle size exceeded 0.25 mm, the dispersion coefficient increased rapidly, with the dispersion coefficient differing by a factor of 202. When the particle size was 0.1–2 mm (i.e., fine sands–gravels), the dispersion coefficient was between 0.152–2.37 cm^2/s, with the difference being a factor of approximately 15. However, when the particle size was greater than 2 mm, the change in the dispersion coefficient with respect to particle size became smaller, with the dispersion coefficient tending to reach a constant value as the particle size increased, finally reaching a value of 2.5 cm^2/s in this test condition. These observations suggest that 0.25 mm and 2 mm could be considered the characteristic particle sizes of coral sands.

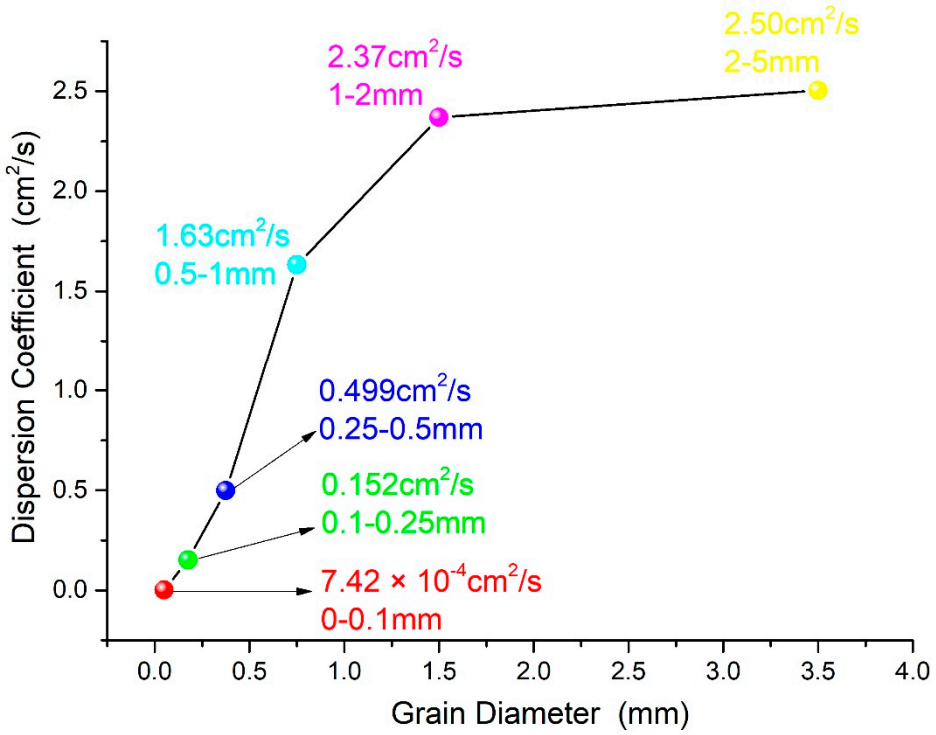

Figure 8. Dispersion coefficients of single-grained soils.

4.2. *Effect of Dry Density on the Dispersion Coefficient*

The effect of the degree of compactness on the one-dimensional dispersion coefficient was investigated using the group of coral sands having a particle size range of 0.25–0.5 mm and dry densities of 1.2 g/cm^3 (relative degree of compactness of 1.021), 1.3 g/cm^3 (relative degree of compactness of 1.212), and 1.4 g/cm^3 (relative degree of compactness of 1.375). The test results, which are shown in Figure 9, indicate that with the increase in density, the displacement stage became longer, the diffusion rate decreased, and the time spent before reaching a steady state increased. Figure 10 represents the variation of the dispersion coefficient with the change in dry density, which reveals that the dispersion coefficient decreased linearly with increasing dry density.

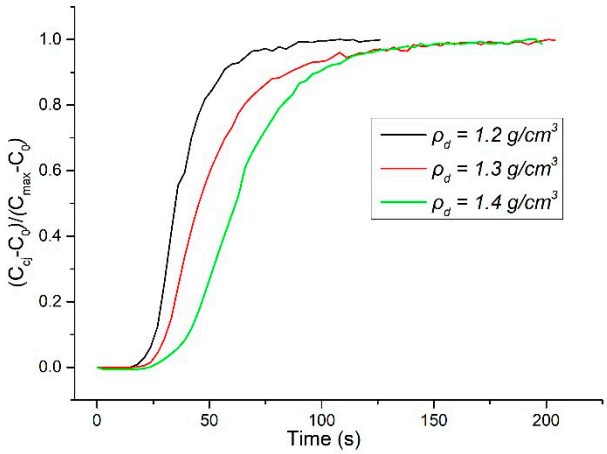

Figure 9. One-dimensional dispersion curves of coral sands with different dry densities.

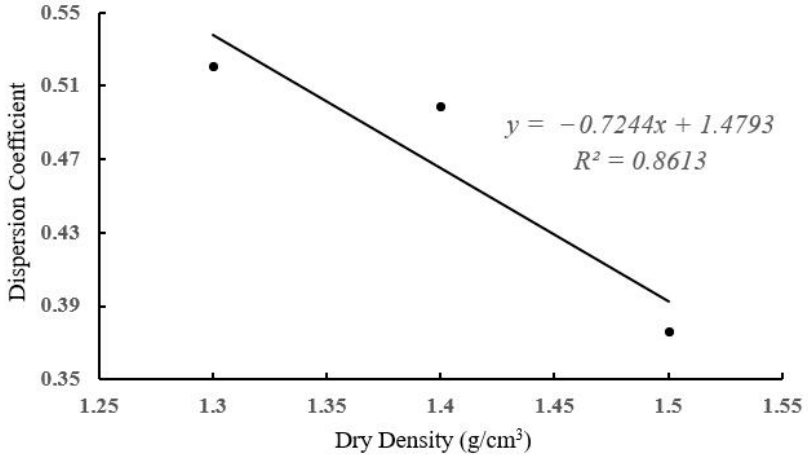

Figure 10. One-dimensional diffusion coefficients of coral sands with different dry densities.

4.3. Effect of Particle Gradation on the Dispersion Coefficient

To simulate natural-gradation sands, stepwise removal of the particles smaller than a certain size was conducted in order to change the gradation [17]. This was followed by one-dimensional dispersion tests on coral sands of different gradations to investigate the effect of particle gradation on the one-dimensional dispersion coefficient. The sample dry density was 1.3 g/cm^3 and the gradation parameters of each sample are listed in Table 2 [18]. As shown by the data, all the samples were poorly graded coral sands, with the exception of the natural gradation sands. The gradation curves of the samples are displayed in Figure 11 and the dispersion coefficient curves are illustrated in Figure 12.

Table 2. Gradation parameters of the samples.

Sample	d_{60}	d_{30}	d_{10}	C_c	C_u
No. 1	2.5	0.52	0.05	2.163	50.000
No. 2	2.5	0.52	0.15	0.721	16.667
No. 3	2.5	0.6	0.31	0.465	8.065
No. 4	2.5	0.9	0.6	0.540	4.167
No. 5	2.55	1.5	1.2	0.735	2.125

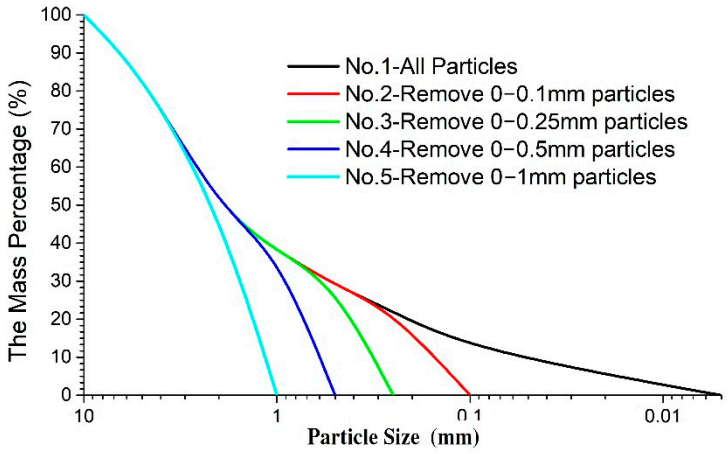

Figure 11. Gradation curves of the samples.

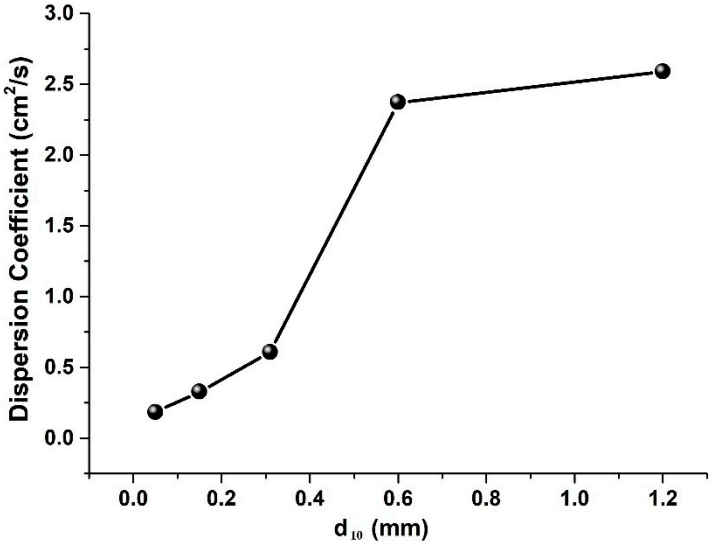

Figure 12. One-dimensional dispersion coefficients of samples with different gradations.

As shown in Figure 12, the dispersion coefficient of the coral sands gradually increased with increasing d_{10}. Following the removal of soil particles smaller than 0.25 mm (d_{10} increased to 0.31 mm from the initial 0.05 mm), the dispersion coefficient of the coral sands increased dramatically. After removal of the soil particles smaller than 0.5 mm (d_{10} exceeded 0.6 mm), the dispersion coefficient of the coral sands tended to reach a constant value. These results suggest that 0.25 mm and 2 mm were the characteristic particle sizes for the dispersion properties of graded coral sands.

5. Analysis of the Dispersion Mechanisms in Coral Sands

There are many significant factors affecting solute transport, such as convection, mechanical dispersion, molecular diffusion, interactions between the solid phase and solute (such as dissolution and adsorption), chemical reactions within the solution, and other source–sink solute interactions (such as attenuation of radioactive elements and absorption of certain solutes by crop roots) [19]. Among these, mechanical dispersion and molecular diffusion are collectively referred to as dispersion. Studies have shown that mechanical dispersion and molecular diffusion generally occur simultaneously during solute transport, although they exhibit different variation patterns with changing average pore flow velocity. When the flow velocity is low, molecular diffusion is stronger than mechanical dispersion. In contrast, when the flow velocity is high, mechanical dispersion is stronger than molecular diffusion. In order to reveal the roles of these two mechanisms in the solute dispersion process of coral sands,

pore tortuosity tests, as well as molecular and mechanical dispersion tests, were performed on the coral sands in this study.

5.1. Molecular Diffusion in Coral Sands

Figure 13 depicts a curve showing the diffusion concentrations of solute molecules in coral sands having different particle sizes. E_{NaCl} is the conductivity measured by the left sensor and E_{water} is measured by the right sensor, with $E_{Med} = (E_{NaCl} + E_{water})/2$. When there was a concentration gradient in the saturated porous medium and the pore flow velocity was 0, the NaCl solution concentrations gradually decreased and increased in the left and right samples, respectively, until the two concentrations reached a relative equilibrium. It is noteworthy that the concentrations of the NaCl solution on both sides were not necessarily the same when equilibrium was reached; this was due to the fact that when the concentration gradient was low (defined as the limiting concentration gradient at equilibrium, ranging from 0–1, with larger values representing larger concentration gradients at equilibrium), the "obstruction" effect of the porous medium occurred, and the concentration gradient would not continue to decrease. Porous media with different particle sizes (pore sizes) had different limiting concentration gradients at equilibrium. As shown by Figure 13, when the particle size was larger than 0.1 mm, the time spent prior to reaching the limiting concentration gradient at equilibrium gradually decreased with increasing particle size, concomitant with a gradual decrease in the limiting concentration gradient at equilibrium. When the particle size was larger than 1 mm, the limiting concentration gradient at equilibrium was infinitely close to 0. When the particle size was smaller than 0.1 mm, the molecular driving force generated by the concentration gradient was less than the "obstruction" effect of the porous medium; thus, the limiting concentration gradient at equilibrium was rapidly achieved and relatively large (approaching 1). Figure 14 illustrates how the amount of time taken to reach the limiting concentration gradient at equilibrium varied with particle size. As shown in Figure 14, 0.1–0.25 mm was still the characteristic particle size of coral sands for molecular dispersion, and the group of coral sands with this particle size range took the longest time to reach the limiting concentration gradient at equilibrium. This finding is in agreement with the conclusion drawn from the one-dimensional dispersion test conducted in this study.

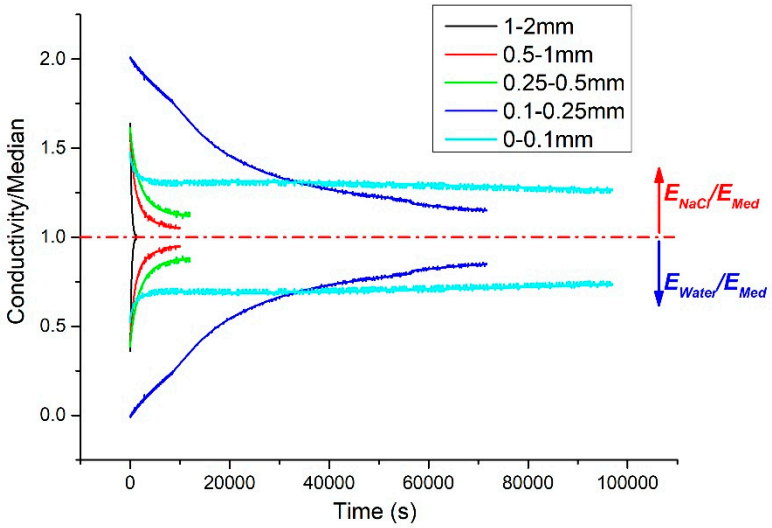

Figure 13. Concentration variation curves during molecular diffusion in coral sands.

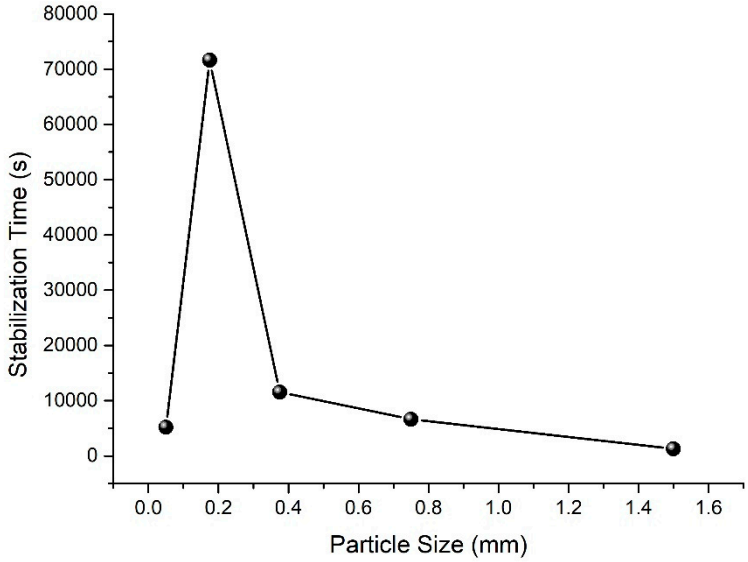

Figure 14. Varying amounts of time required to reach the limiting concentration.

In order to quantitatively characterize the "obstruction" effect of porous media on molecular diffusion, earlier studies introduced the concept of pore tortuosity (θ), i.e., the ratio of the length of the porous medium sample to the actual path traveled by the fluid particles through a sample of that length [20]. Thus, $\theta = D_0/D^*$, where D_0 is the dispersion coefficient in the open water body and D^* is the dispersion coefficient in the porous medium. Given the assumption that the limiting concentration gradient at equilibrium infinitely approaches 0 for molecular diffusion in an open and still water body, the θ of a porous medium should range between 0 and 1. According to the definition of pore tortuosity, $\theta = S/(v \times t)$, S (cm) is the length of the porous medium sample, v (cm/s, taken as scalar without considering direction) is the velocity of fluid particle movement, and t (s) is the time duration of fluid particle movement, namely, the time spent by the fluid particles prior to reaching the limiting concentration gradient at equilibrium. Based on the data in Figure 13, the time t in each particle size group of coral sands could be obtained, with t set to positive infinity in the case of particle sizes less than 0.1 mm. In addition, based on the time t and the known distance of 4.9 cm between the sensor and the central partition, it was possible to obtain the relationship curve of pore tortuosity versus particle size, as shown in Figure 15, where v is the velocity of fluid particle movement at a certain temperature.

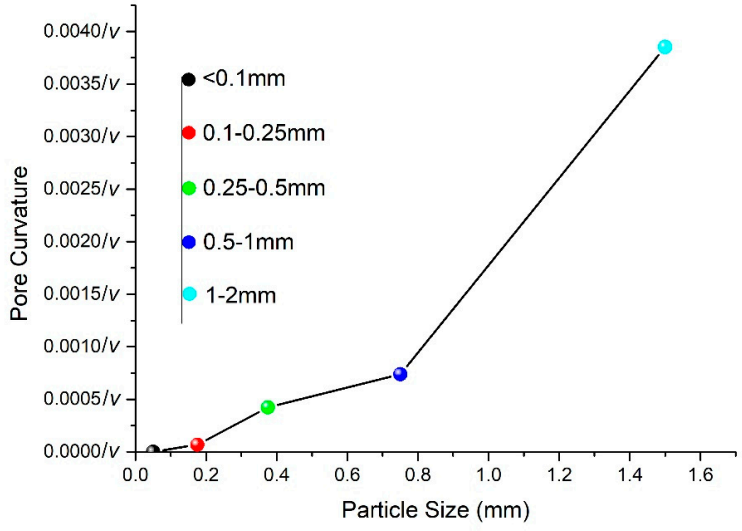

Figure 15. Relationship curve between pore tortuosity and particle size of coral sands.

A previous study on the dispersion characteristics of terrigenous sediments found that θ ranges from 0.01–0.5 [21]. In addition, this parameter has been proposed to be 0.1 for clays and 0.7 for sandy soils [22].

5.2. Mechanical Dispersion in Coral Sands

Dispersion consists of molecular diffusion and mechanical dispersion. When the flow velocity is greater than 0, the two processes usually coexist, albeit with different weights on the overall dispersion coefficient under different conditions (i.e., concentration and flow velocity).

Figure 16 presents the variation curves of relative conductivity at a fixed pore flow velocity of 0 for two different concentrations of tracer NaCl solution (20 g/L versus 60 g/L). Here, E_C is the sensor-measured conductivity, E_0 is the initial conductivity before the injection of the tracer, and E_{max} is the maximum conductivity measured by each sensor. The rate of increase (slope) of relative conductivity was greater for the 60 g/L NaCl solution than for its 20 g/L counterpart, suggesting that the higher the concentration gradient, the greater the molecular diffusion rate.

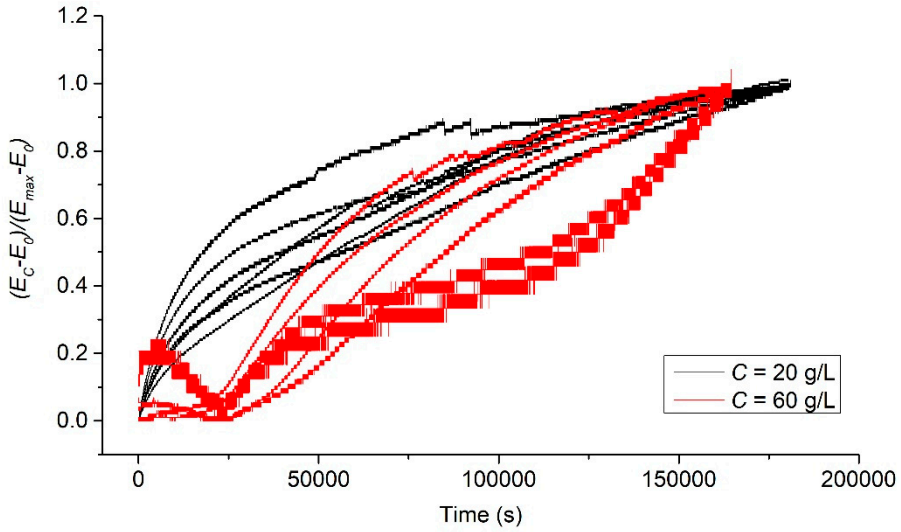

Figure 16. Molecular diffusion curves of different concentration gradients.

Figure 17 shows the variation curves of relative conductivity at different flow velocities, with Figure 17A–D depicting the variation curves of measured conductivities from the sensors EC_1 to EC_3. Figure 17a–d depict the variation curves of measured conductivities from the sensors EC_4 to EC_6. In relation to the tracer injection port, the sensors EC_1 to EC_3 were downstream, while the sensors EC_4 to EC_6 were upstream. The dispersion process downstream from the port would involve both mechanical dispersion and molecular diffusion, with both taking place in the same direction. In contrast, in the dispersion process occurring against the flow direction upstream from the port, mechanical dispersion would take place in a different direction than molecular diffusion. Therefore, the conductivity change detected by the sensor would be a net conductivity change of the solutes with their molecular diffusion overcoming their mechanical dispersion. Generally, when mechanical dispersion dominates, the shape of concentration–time curve will be as shown in Figure 18a. In this situation, concentration attenuation occurs after the maximum concentration has been reached, with t_p denoting the time taken to reach the peak point of the curve. When molecular diffusion dominates, the shape of the concentration–time curve is as shown in Figure 18b. In this case, the concentration remains constant after reaching the maximum value, with t_s denoting the time taken to reach the stable point of the curve.

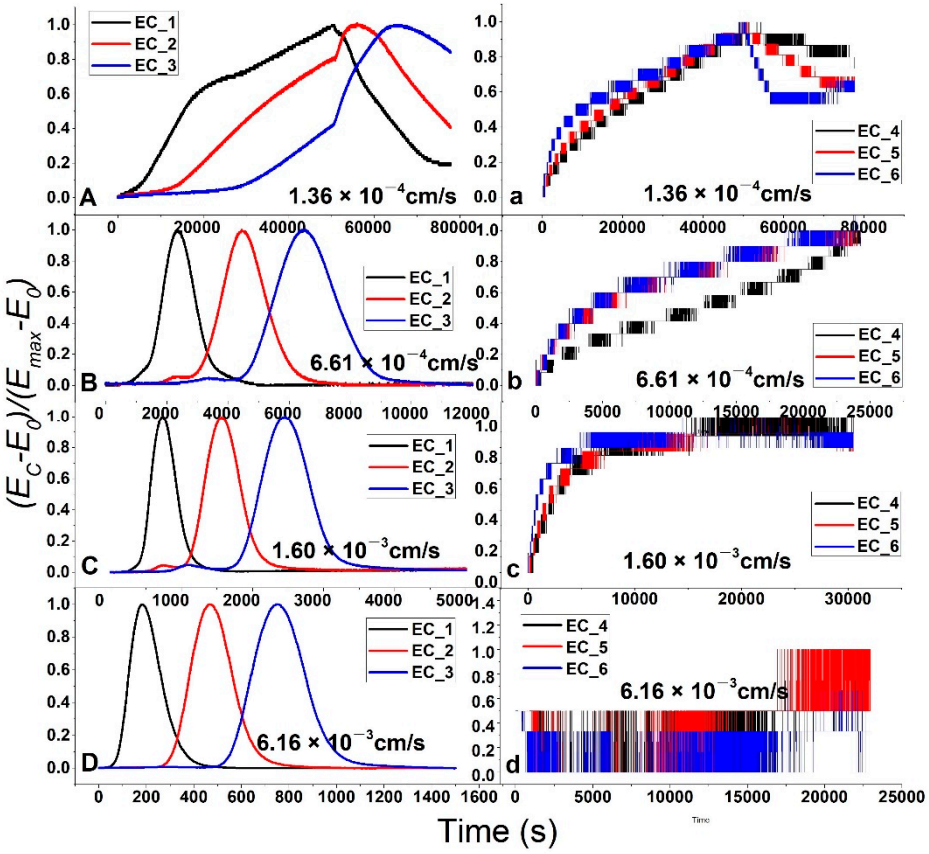

Figure 17. Dispersion mechanisms in coral sands having different pore flow velocities. (Figure 17A–D depicting the variation curves of measured conductivities from the sensors EC_1 to EC_3. Figure 17a–d depict the variation curves of measured conductivities from the sensors EC_4 to EC_6.)

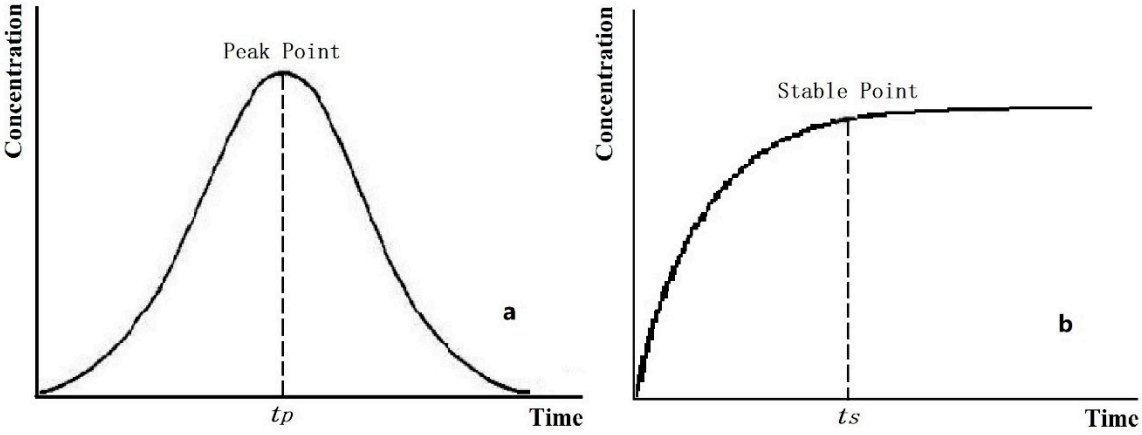

Figure 18. Schematic of the typical curves corresponding to different dispersion mechanisms.

It can be seen that when the flow velocity was 1.36×10^{-4} cm/s (Figures 17A and 17a), the curve characteristics of the left figure fell between those of Figures 18a and 18b, indicating the simultaneous presence of the two mechanisms of molecular diffusion and mechanical dispersion downstream from the port. Data comparison between the left and right figures indicates that the time to reach the maximum conductivity was similar in the two figures, suggesting that the two mechanisms were comparable in terms of the dispersion process under this condition. The relative conductivity decreased

after the peak value in the right figure, which was likely the result of the displacement effect of the pore fluids.

With the increase in flow velocity, the curve shape in the left figure (Figure 17A–D) becomes gradually similar to that in Figure 18a, indicating that mechanical dispersion was gradually enhanced. This was manifested by the gradual shortening of the displacement stage and the continuous increase in the diffusion rate. In contrast, the curve shape in the right figure (Figure 17a–d) became increasingly atypical, and the time taken to reach the maximum value gradually increased and was much longer than the corresponding time in the left figure, indicating that molecular diffusion was increasingly subject to the flow velocity. By the time the flow velocity reached 6.16×10^{-3} cm/s, the molecular diffusion upstream from the tracer injection port was basically negligible.

Based on a comprehensive analysis of the above test results, the velocity boundaries of the pore fluids that control the dispersion mechanisms were derived, as shown in Table 3.

Table 3. Velocity threshold value of pore fluids that control the dispersion mechanisms.

Classification	Existing Classification Method [21]	Classification Method in This Study (flow velocity u, cm/s)	Description
I	Very low flow velocity	u approaching 0	Molecular diffusion dominates, while mechanical dispersion is negligible
II	Flow velocity increasing	$0 < u < 1.36 \times 10^{-4}$	The two types of diffusion are comparable
III	Flow velocity continuing to increase	$1.36 \times 10^{-4} < u < 1.60 \times 10^{-3}$	Mechanical dispersion dominates, while molecular diffusion is weak
VI	Higher flow velocity	$1.60 \times 10^{-3} < u < 6.16 \times 10^{-3}$	Mechanical dispersion dominates, while molecular diffusion is negligible
V	Flow velocity too high	$u > 6.16 \times 10^{-3}$	Turbulence and inertial forces weaken mechanical dispersion

6. Conclusions

The solute diffusion coefficient of coral sands is a key factor affecting fresh groundwater conservation, and knowledge of the freshwater dispersion pattern in coral sands will provide both the basic parameters and a theoretical basis for numerical simulation of the formation and evolution of freshwater aquifers under islands, as well as the conservation and utilization of these aquifers. Using coral sands collected from a reef in the South China Sea, a series of tests and theoretical analyses were conducted in this study, from which the following conclusions were drawn:

1) The particle size of coral sands was an important parameter affecting the dispersion coefficient, which increased with increasing particle size. The reason is that when the volume and porosity of the soil are constant, the number of pores decreased and the pore size increased with the increase in particle size. Because the pore fluid was more likely to mechanically flow in larger pores, the diffusion coefficient, therefore, could increase. The diameters of 0.25 mm and 2 mm were discovered to be the characteristic particle sizes of coral sands due to their dispersion characteristics. The dispersion coefficient could vary by a factor of more than 200 between the 0.1–0.25 mm size group and the 0.25–0.5 mm size group, while the dispersion coefficient increased at a relatively small rate in the group with particle sizes larger than 2 mm.
2) Gradation was also an important factor affecting the dispersion coefficient of coral sands, with the diffusion coefficient increasing with increasing d_{10}. When d_{10} was larger than 0.31 mm, the dispersion coefficient increased dramatically. In contrast, when d_{10} was larger than 0.6 mm, the dispersion coefficient tended to be constant. This was because an increase in d_{10} reflected that the filling degree of the fine particles in the soil became worse. Similarly, the pore size and diffusion coefficient increased with an increase in d_{10}. However, when d_{10} was 0.31 mm or less, the diffusion coefficient did not increase with increasing d_{10}. The reason was the increase in pore

size was minimal with respect to the macroscopic scale. Alternatively, the importance of pore size for the macro scale grew with an increase in d_{10}, and the diffusion coefficient also rose. Finally, when the pore size reached a critical value, the influence of pore size on the solute diffusion gradually reduced, and the diffusion coefficient also approached a stable state.

3) The dispersion coefficient of coral sands decreased linearly with an increasing degree of compactness. The dispersion coefficient decreased at a rate of −0.7244 in the group of coral sands with particle sizes of 0.25–0.5 mm. The reason was that when the particle size distribution remained stable, the increase in compactness directly resulted in a decrease in porosity, which could restrict the flow of the pore liquid. The diffusion coefficient, therefore, was reduced. By analyzing the experimental dates, the diffusion coefficient was reduced when the dry density was increased from 1.3 g/cm^3 to 1.5 g/cm^3.
4) Both the concentration of solute in the coral sands and the particle size of the porous medium affected the limiting concentration gradient at equilibrium. With an increase in solute concentration and particle size, the limiting concentration gradient at equilibrium decreased. As particle size increased, the pore tortuosity decreased. This was because when the soil volume and porosity were constant, the number of pores decreased and the pore size increased with an increase in the particle size, and the actual distance that the solution molecules flowed from point A to point B in the soil was shortened. Therefore, the calculated porosity curvature was reduced.
5) The dispersion mechanisms in coral sands could be determined by the flow velocity of the pore fluid. Based on the different weights of molecular diffusion versus mechanical dispersion for different conditions of flow velocity, the dispersion mechanisms could be classified into five types.

Author Contributions: Conceptualization, X.C., C.Z., M.H. and X.W.; Data curation, X.C. and H.L.; Formal analysis, X.C.; Funding acquisition, C.Z., M.H. and X.W.; Project administration, C.Z. and M.H.; Resources, X.W. and H.L.; Writing—original draft, X.C.; Writing—review and editing, C.Z.

Funding: This research was funded by the National Natural Science Foundation of China (Grant Nos. 41877271, 41372318, 41330642, and 41572304) and the Strategic Pilot Science and Technology Special Foundation of Chinese Academy of Sciences (Grant Nos. XDA13010300).

Conflicts of Interest: The authors declare no conflict of interest.

References

1. Hu, M.; Cui, X.; Wang, X.-Z.; Liu, H.; Zhang, C. Experimental study on the effect of fine particles on permeability of the calcareous sand. *Rock Soil Mech.* **2019**, *40*, 1–6.
2. Zhu, C.; Zhou, B.; Liu, H. State-of-the-art review of developments of laboratory tests on cemented calcareous soils. *Rock Soil Mech.* **2015**, *36*, 311–319.
3. Zhu, C.; Zhou, B.; Liu, H. Micro-structures and fundamental engineering properties of beach calcarenite from south china sea. *Chin. J. Rock Mech. Eng.* **2015**, *34*, 683–693.
4. Zhu, C.; Chen, H.; Meng, Q.; Wang, R. Microscopic characterization of intra-pore structures of calcareous sands. *Rock Soil Mech.* **2014**, *35*, 1831–1836.
5. Taylor, G. Dispersion of Soluble Matter in Solvent Flowing Slowly through a Tube. *Math. Phys. Sci.* **1953**, *219*, 186–203.
6. Klotz, D.; Moser, H.; Neumaier, F. Dispersivity and velocity relationship from laboratory and field experiments. *J. Hydrol.* **1980**, *45*, 169–184. [CrossRef]
7. De Gennes, P.G. Hydrodynamic dispersion in unsaturated porous media. *J. Fluid Mech.* **1983**, *136*, 189–200. [CrossRef]
8. De Arcangelis, L.; Koplik, J.; Redner, S. Hydrodynamic Dispersion in Network Models of Porous Media. *Phys. Rev. Lett.* **1986**, *57*, 8. [CrossRef] [PubMed]
9. Muhammad Sahimi, I. Fractal and Superdiffusive Transport and Hydrodynamic Dispersion in Heterogeneous Porous Media. *Transp. Porous Media* **1993**, *13*, 3–40. [CrossRef]
10. Lowe, C.P.; Frenkel, D. Do Hydrodynamic Dispersion Coefficients exist. *Phys. Rev. Lett.* **1996**, *77*, 4552–4555. [CrossRef] [PubMed]

11. Zhang, F.; Kang, S.; Pan, Y. Experimental study on hydrodynamic dispersion of adsorption solute in saturated-unsaturated soil. *J. Hydraul. Eng.* **2002**, *3*, 84–90.
12. Li, L.; Zhu, W.; Qu, Y. Experiment study on hydrodynamic dispersion parameters for contaminated soil with low permeability. *Chin. J. Geotech. Eng.* **2011**, *33*, 1308–1312.
13. Shao, A.; Liu, G.; Yang, J. In-lab determination of soil hydrodynamic dispersion coefficient. *Acta Pedol. Sin.* **2002**, *39*, 184–189.
14. Hogh, K.; Jensen, G.; Destouni, M. Advection-dispersion analysis of solute transport in undisturbed soil monoliths. *Ground Water* **1996**, *34*, 1090–1097.
15. Zheng, C.; Gordon, B. *Applied Contaminant Transport Modeling*; Higher Education: Beijing, China, 2009.
16. Ministry of Construction of the People's Republic of China. *GB 55021—2001 Code for Investigation of Geotechnical Engineering*; China Building Industry: Beijing, China, 2009.
17. Xie, D.; Cai, H.; Wei, Y.; Li, W. Scaling principle and method in seepage tests on coarse materials. *Chin. J. Geotech. Eng.* **2015**, *37*, 369–373.
18. Ministry of Water Resources of the People's Republic of China. *GB/T 50123—1999 Standard for Geotechnical Test Methods*; China Planning: Beijing, China, 1999.
19. Qian, H.; Ma, Z. *Hydrogeochemistry*; Geological Publishing House: Beijing, China, 2005.
20. Bear, J. *Dynamics of Fluids in Porous Media*; Elsevier: New York, NY, USA, 1972; 764p.
21. Freeze, R.A.; Cherry, J.A. *Groundwater*; Prentice Hall: Englewood Cliffs, NJ, USA, 1979; 604p.
22. Konikow, L.F.; Bredehoeft, J.D. Ground-water models cannot be validated. *Adv. Water Resour.* **1992**, *15*, 75–83. [CrossRef]